Invited paper

ELECTRICAL IMPEDANCE TOMOGRAPHY – FROM THE BASICS TO RECENT ADVANCES

Kostadin BRANDISKY[1]

Abstract: The paper reviews the basics and the recent advances in Electrical Impedance Tomography (IET). The problems arising in the forward and inverse problems in 2D and 3D EIT are considered, as well as the instrumentation needed to collect measurement data for the image reconstruction.

Keywords: Electrical Impedance Tomography, Numerical Methods, Computational Electromagnetics

1. INTRODUCTION

Electrical Impedance Tomography is an image reconstruction technique that allows tomographic images to be obtained inside a body by using voltage or current measurements on its surface [1,4]. Usually small currents are injected using electrodes applied on the surface of the body, and the presence of inhomogeneities inside the body causes specific distribution of electric potential to appear on the surface. To find what conductivity distribution causes such potentials on the surface, an inverse problem is solved.

Application of this technique can be found in several fields [4]:

- Medical imaging – monitoring the lungs and heart function, blood flow, brain inspection, mammography – screening for breast cancer.
- Geophysical prospecting – finding mineral deposits in the earth, finding lost mine galleries, finding burried metallic objects (landmines) or objects of historic importance.
- Industrial applications – imaging multiphase fluid flows, monitoring pipes for clustering of materials, non-destructive testing and finding defects in machine parts.

In this paper the use of Electrical Impedance Tomography for medical imaging is considered. In this field EIT has several advantages, compared to other imaging methods (e.g. X-Ray tomography) [2]: (i) it is a non-invasive and non-destructive method that can be used for longer periods of monitoring the patient's state; (ii) it is relatively inexpensive; (iii) EIT can provide information for electrical properties of the tissues that cannot be provided by other techniques.

The major drawback of the EIT is its relatively small spatial resolution (in order of 10 % of the image diameter). This is due to practical difficulties of applying large number of electrodes to the body, and the need of complex electronic instrumentation to measure signals with large dynamic range.

From mathematical point of view, the reconstruction of the conductivity distribution by EIT leads to non-linear ill-posed inverse problems [3], because the changes of the material properties inside the body produce small changes of the potentials on the surface. High-precision data acquisition techniques and accurate reconstruction algorithms are necessary to solve such inverse problems. A lot of work on this subject has been done, and it can be seen that with the availability of affordable but powerful personal computers and parallel multiprocessor computers some sophisticated algorithms are again on the forefront of the research, allowing even high quality imaging of 3D bodies.

The research in the field of EIT is continuing for some 30 years, but there are only several commercial EIT systems available on the market. There are two reasons for this [3]:

- The existing reconstruction algorithms require lengthy calculations, which have to be performed in real-time in order to ensure 20-30 frames/per second, necessary for biomedical monitoring. This problem is less important for the industrial applications, where the objects are still and do not change their parameters.
- The measurement of the potentials on the boundaries requires precision instrumentation. High precision measurement systems are necessary to track the small changes of the boundary potentials, caused by the changes of the conductivities inside the body. This requires very miniature electrodes and computer controlled high-precision analog to digital converters, capable to deliver precision of $0.1 \div 0.01$ %.

The solution of the inverse problem of reconstructing the conductivities consists of repeated solutions of the forward problem – that finds the distribution of electric field inside the body of interest, and adapting the conductivities till the computed potentials on the boundary converge to the measured potentials with pre-specified accuracy.

In this paper, first, the solution of the forward problem will be considered briefly. This solution is essential component of EIT. Nowadays advanced numerical methods, as the finite element method and the boundary element method are popular with their accuracy and flexibility. Next, the most popular Gauss-Newton reconstruction algorithm, based on iterative solution of non-linear systems of equations, will be considered. Then, a description of a typical instrumentation system for EIT will be done, together with the hardware requirements. At the end, the

[1] Technical University of Sofia, 8, Kliment Ohridski Blvd., Sofia 1000, Bulgaria, E-mail: kbran@tu-sofia.bg

recent advances and perspectives of EIT will be briefly discussed.

2. MATHEMATICAL MODEL

2.1 Governing equations

In EIT for medical imaging AC currents are used in order to avoid polarization effects. Their frequency range is usually less than 1 MHz. For safety reasons the rms value of the excitation current does not exceed 1÷5 mA. For such comparatively low frequencies, the assumption of static fields can be used (ω = 0). In these conditions the Maxwell equations are reduced to the following partial differential equation:

$$\nabla \cdot (\sigma \nabla V) = 0 \tag{1}$$

Here the electric potential V is a scalar function and the conductivity σ is real valued.

If both the amplitude and phase angle of the boundary voltages are measured, the electrical conductivity and permittivity distributions in the interior of the volume can be found. At low frequencies, the phase angles of the voltages are relatively small. In the absence of phase angles in the data, only the conductivity distribution can be reconstructed and the technique is called Electrical Resistance Tomography (ERT).

Because the frequency range in EIT in some cases exceeds 1 MHz, neglecting the capacitive effects can cause inaccuracies. A variant of the quasi-static approximation, in which the capacitive effects are taken into account, can be obtained by accepting time-harmonic field in linear and isotropic media. This can be done at the assumption, that magnetic induction is negligible (because the applied currents are of order of 1 mA, and the magnetic permeability of the tissues is very low). This gives the equation

$$\nabla \cdot (\sigma + j\omega\varepsilon)\nabla \dot{I} = 0 \tag{2}$$

where ε is permittivity and σ is conductivity of the medium, ω is the angular frequency of the excitation current. This is a more general approach, which allows imaging of both conductivity σ and permittivity ε distributions. This technique is generally called Electrical Impedance Tomography (EIT).

At high frequencies (f > 10 MHz) and low conductivities of the media (i.e., in dielectric objects), the distribution of permittivity ε can be found - this method is called Electrical Capacitance Tomography (ECT) and is mostly used in industrial imaging.

Here, for brevity, only the imaging of σ will be considered and Eq. (1) will be used.

Equation (1) must be solved in the region of interest together with the following boundary condition:

$$\sigma \frac{\partial V}{\partial n} = \mathbf{J}_{\mathbf{n}}^{\mathbf{s}} \text{ on } \delta\Omega \tag{3}$$

2.2 Solution of the forward problem

The most commonly used method for solving the forward problem in EIT is the Finite Element Method (FEM) [6]. It consists in forming and solving a sparse linear system of equations. This system is symmetric and positive definite, which allows efficient sparse matrix methods to be used for its solution. In EIT, in order to collect more independent measurement data, several current excitation patterns are used (usually $n/2$, where n is the number of electrodes). The finite element equations are formed and solved for each current pattern, in the form:

$$\mathbf{Ax} = \mathbf{y} \tag{4}$$

where $\mathbf{A}$ is the $r \times r$ symmetric global matrix evaluated at conductivity distribution $\boldsymbol{\sigma}^{\mathbf{k}}$, and $\mathbf{x}$ and $\mathbf{y}$ are r-dimensional vectors, which hold the nodal voltages and currents, respectively. The finite element mesh contains r nodes and the FEM system of equations is solved for the nodal voltages of all r nodes. The well-known Cholesky method is the standard approach of solving the system in Eq. (4). The Cholesky decomposition factors $\mathbf{A}$ into the form $\mathbf{LL}^{\mathbf{T}}$, where $\mathbf{L}$ is lower triangular matrix, so Eq. (4) becomes:

$$\mathbf{LL}^{\mathbf{T}}\mathbf{x} = \mathbf{y} \tag{5}$$

The following triangular systems are then solved by forward and backward substitution:

$$\mathbf{Lu} = \mathbf{y} \tag{6}$$

$$\mathbf{L}^{\mathbf{T}}\mathbf{x} = \mathbf{u} \tag{7}$$

Since during the solution new nonzero elements arise (called fill-ins), their reduction is desirable as it leads to fewer floating point operations when using sparse matrix techniques to solve the equations.

The sparse matrix solution of the finite element equations can be divided into the 3 steps shown in Fig. 1.

- Symbolic factorization
- Numerical factorization
- Forward and backward substitution

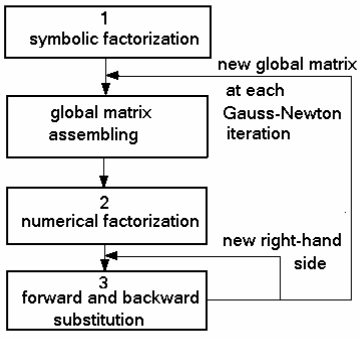

Fig. 1 - *Sparse matrix solution*

For each repeated solution at different projection angle (current pattern), the right hand side vector is only changed, so neither the global matrix assembly nor factorization is repeated because the structure of the global matrix is the same for the same finite element mesh. The first step (symbolic factorization) is performed only once for any number of Gauss-Newton iterations. It includes

also node renumbering using minimum degree algorithm, nested dissection ordering or Reverse Cuthill-McKee algorithm.

2.3 The Gauss-Newton method

The Gauss-Newton method [8] (also called modified Newton-Raphson method) is iterative method which solves for the conductivity distribution at given measured voltages and current excitations. It uses a FEM solver to solve the forward problem of finding the potential distribution at given conductivity distribution and current excitation pattern. It updates iteratively the conductivity distribution till a pre-specified error between the measured and computed potentials on the electrodes is attained. For this purpose, a vector $\mathbf{V_0}$ is defined containing $n \times p$ measured voltages for p projection angles, and a vector $\mathbf{V(\sigma)}$ is created, containing $n \times p$ electrode voltages for all projection angles, computed using FEM at conductivity distribution $\boldsymbol{\sigma}$ ($\boldsymbol{\sigma}$ is a vector of length *m,* the number of finite elements in the mesh). Next, an objective function ϕ is defined, representing the error between $\mathbf{V(\sigma)}$ and $\mathbf{V_0}$:

$$\phi = \frac{1}{2}\left(\mathbf{V}(\boldsymbol{\sigma}) - \mathbf{V_0}\right)^T \left(\mathbf{V}(\boldsymbol{\sigma}) - \mathbf{V_0}\right) \tag{8}$$

Minimization of this error with respect to the conductivity gives:

$$\phi' = \left[\mathbf{V}'(\boldsymbol{\sigma})\right]^T \left[\mathbf{V}(\boldsymbol{\sigma}) - \mathbf{V_0}\right] = 0 \tag{9}$$

The matrix

$$\mathbf{J} = \left[\mathbf{V}'(\boldsymbol{\sigma})\right] = \frac{\partial \mathbf{V}}{\partial \boldsymbol{\sigma}} \tag{10}$$

is called *Jacobian* and is $np \times m$ rectangular matrix (n is the number of electrodes, p is the number of projection angles and m is the number of finite elements with different conductivities). An element of this matrix $J_{i,j} = \partial V_i / \partial \sigma_j$ is the partial derivative of the electrode voltage V_i against the conductivity σ_j of element j.

Finding the Taylor expansion of (9) and ignoring the higher order terms, the following correction to the conductivity at k-th iteration is found:

$$\Delta\boldsymbol{\sigma}_k = -\left[\mathbf{J}_k^T \mathbf{J}_k\right]^{-1} \left[\mathbf{J}_k^T \left(\mathbf{V}(\boldsymbol{\sigma}_k) - \mathbf{V_0}\right)\right] \tag{11}$$

The conductivity update $\Delta\boldsymbol{\sigma}_k$ for each iteration step k of the non-linear algorithm is obtained by solving the following linear system of equations:

$$\left(\mathbf{J}_k^T \mathbf{J}_k\right) \Delta\boldsymbol{\sigma}_k = -\mathbf{J}_k^T \left(\mathbf{V}(\boldsymbol{\sigma}_k) - \mathbf{V_0}\right) \tag{12}$$

The updated conductivity distribution at iteration k is found by:

$$\boldsymbol{\sigma}_{k+1} = \boldsymbol{\sigma}_k + \Delta\boldsymbol{\sigma}_k \tag{13}$$

When the iteration step produces changes of the conductivity $\boldsymbol{\sigma}_k$ that are smaller than some predetermined tolerance or correspondingly small changes in ϕ, it is said that the iterative procedure has converged and can be stopped.

In some recent publications [7] the objective function to be minimized is constructed using the *goodness of fit factor*, measured by the χ^2 *-statistics*:

$$\chi^2 = \sum_i^{np} \left(\frac{V_{i(\sigma)} - V_{i(o)}}{\delta V_i} \right)^2 \tag{14}$$

where: $V_{i(\sigma)}$ - measured signal; $V_{i(o)}$ – computed signal on the electrodes at specific distribution of σ; $\delta\mathbf{V}$ - irreducible random noise contribution to the measured signal. The criterion for adequate fit is $\chi^2 < M$, where M is the number of independent measurements ($M = n \times p$). The following flow chart describes the algorithm of the Gauss-Newton method:

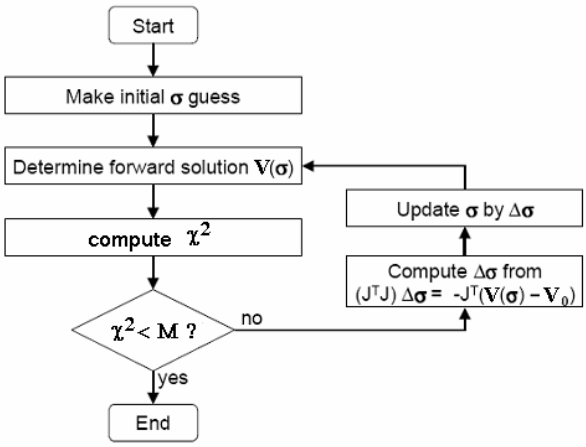

Fig. 2 - *Flow chart of the Gauss-Newton method*

2.4 Computation of the Jacobian

The Jacobian used in (11) can be computed in several ways. The first one is called *standard method* [8]. It is based on the finite element solution used for the forward problem. After generation of the finite element mesh the following matrix equation is obtained:

$$\mathbf{A}\,\mathbf{x} = \mathbf{b} \tag{15}$$

The j-th column of the Jacobian can be obtained by differentiating the solution $\boldsymbol{x}$ of the system (15) with respect to the conductivity σ_j :

$$\frac{\partial \mathbf{x}}{\partial \sigma_j} = \frac{\partial \left(\mathbf{A}^{-1}\mathbf{b}\right)}{\partial \sigma_j} \tag{16}$$

The right hand side of (16) can be represented as

$$\frac{\partial \left(\mathbf{A}^{-1}\mathbf{b}\right)}{\partial \sigma_j} = -\mathbf{A}^{-1} \frac{\partial \mathbf{A}}{\partial \sigma_j} \mathbf{A}^{-1}\mathbf{b} = -\mathbf{A}^{-1} \frac{\partial \mathbf{A}}{\partial \sigma_j} \mathbf{x} \tag{17}$$

in which the derivative $\partial \mathbf{A} / \partial \sigma_i$ has elements

$$\frac{\partial A_{m,i}}{\partial \sigma_j} = \int_{\Delta_j} \nabla \varphi_m \cdot \nabla \varphi_i \tag{18}$$

The matrix $\partial \mathbf{A}/\partial \sigma_j$ is very sparse. It contains only the contributions from the *j*-th element matrix, without being multiplied by σ_j. This matrix has to be multiplied by the solution vector **x**, containing nodal potentials. The result will be a column vector that has non-zeroes only in those rows that correspond to node numbers of the *j*-th element. The already factored matrix $\mathbf{A}^{-1}$ (in the forward solution), can be used to solve a new system, which solution will be the derivatives of all potentials with respect to the conductivity of the *j*-th element. Since (16) forms the derivatives of all potentials, the part which belongs to the electrodes has to be extracted.

The Jacobian matrix is a $np \times m$ partitioned matrix (*n* is number of electrodes, *p* is the number of projection angles, *m* is the number of elements), the structure of which is shown in Fig. 3. Each partition corresponds to a projection angle. The Jacobian is comprised of *mp* *n*-dimensional vectors, $\mathbf{J_{ij}}$ as shown in Fig. 3.

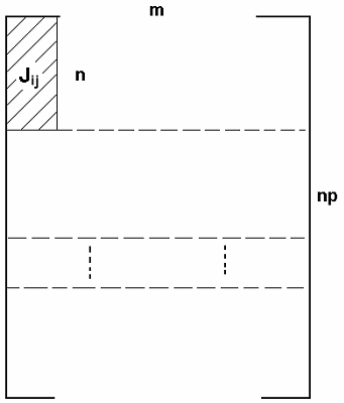

Fig. 3 - *Jacobian matrix structure showing one* $\mathbf{J_{ij}}$ *vector and p partitions*

A more efficient method to obtain the Jacobian is to form the $\mathbf{J_{ij}}$ vector directly [6], avoiding the calculation of the unwanted elements in $\partial \mathbf{x}/\partial \sigma_j$. In Eq. (17), only *n* rows out of the *r* calculated are needed. Substantial savings are possible as $n << r$ when using grids with large numbers of elements. Eq. (17) is modified to calculate $\mathbf{J_{ij}}$ directly

$$\mathbf{J_{ij}} = -\mathbf{G}\frac{\partial \mathbf{A}}{\partial \sigma_j}\mathbf{x_i} \tag{19}$$

where **G** is a $n \times r$ matrix containing just the required *n* rows of $\mathbf{A}^{-1}$ to form $\mathbf{J_{ij}}$. As $\mathbf{A}^{-1}$ is a symmetric matrix, **G** can be formed from either the columns or the rows of $\mathbf{A}^{-1}$. Columns can be obtained efficiently through forward and backward substitution of the equation $\mathbf{A}\mathbf{A}^{-1} = \mathbf{I}$, where **I** is $r \times r$ identity matrix. Only the required columns in $\mathbf{A}^{-1}$ to form **G** are solved for. The factored matrix of **A** is obtained during the finite element equation calculation and is re-used here for the solution of **G** for all projection angles. Re-use for all projections is only possible if the grounded node is kept in the same position for each projection, i.e. the essential boundary conditions are kept constant, and the mesh is the same. The optimal current patterns usually keep the reference node fixed and apply current to all other electrodes.

If maximum unique information is required, then *p=n/2* projections must be used, where *n* is the total number of electrodes. With 2-points current injection, the rows in **G** that relate to the two current carrying electrodes are not used and *n-2* electrode rows are used.

The matrix $\left(\mathbf{J}^{\mathrm{T}}\mathbf{J}\right)$ in (11) is called Hessian. It is a symmetric positive definite matrix of size $m \times m$. This matrix is ill-conditioned. Thus, regularization techniques are required, if images are to be reconstructed from real data which include measurement errors. Usually, the Tikhonov regularization is recommended [6]. In this case the following matrix equation is solved:

$$\boldsymbol{\sigma}_{k+1} = \boldsymbol{\sigma}_k + \left(\mathbf{J}_k^T\mathbf{J}_k + \alpha^2\mathbf{L}^{\mathrm{T}}\mathbf{L}\right)^{-1}\left[\ \mathbf{J}_k^T\left(\mathbf{V_0} - \mathbf{V}\left(\boldsymbol{\sigma}^{\mathrm{k}}\right)\right) + \right. \\ \left. + \alpha^2\mathbf{L}^{\mathrm{T}}\mathbf{L}\left(\boldsymbol{\sigma}_{ref} - \boldsymbol{\sigma}_k\right)\ \right] \tag{20}$$

where **L** is a matrix approximation of a partial differential operator and $\boldsymbol{\sigma}_{ref}$ is a referrence conductivity.

Two other regularization approaches are also used because of their simplicity:

- Diagonal weighting - the regularization matrix is the diagonal weighted matrix $diag\left(\mathbf{J}^{\mathrm{T}}\mathbf{J}\right)$:

$$\Delta\boldsymbol{\sigma}_k = \left(\mathbf{J}_k^T\mathbf{J}_k + \alpha\ diag\left(\mathbf{J}_k^T\mathbf{J}_k\right)\right)^{-1}\mathbf{J}_k^T\left(\mathbf{V_0} - \mathbf{V}\left(\boldsymbol{\sigma}^{\mathrm{k}}\right)\right) \tag{21}$$

- Unit matrix weighting - instead of a weighted diagonal matrix, a weighted unit matrix is used.

In the last years the total variation regularization (TV) is recommended and used [4,11].

3. EIT INSTRUMENTATION

In most of the EIT systems, small AC currents of order of 1÷5 mA rms value are injected through current electrodes and voltages are measured on separate voltage electrodes. The general structure of an EIT system is shown in fig. 4:

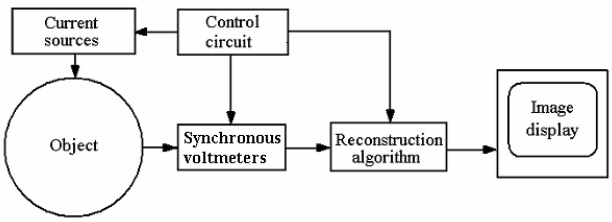

Fig. 4 - *An EIT measurement system*

The EIT systems can be classified according to the number of current sources [4]: (i) single source systems; (ii) multiple sources systems. The waveform used in these systems is a sinusoid, produced by a waveform synthesis circuit. The waveform is fed to a dual current source (or *n* current sources). The currents are supplied to the electrodes through shielded cables in which a driven shield is used to protect the signals from noise, as well as to minimize the cable capacitance. Electrode voltages are measured using synchronous voltmeters. When

using a single voltmeter, it has to be multiplexed to measure all electrode voltages. Using more voltmeters (up to *n)* allows parallelism that reduces measurement time at the expense of more hardware. In general, the voltmetering process is performed synchronously, requiring time reference and reference waveform from the waveform synthesis block. In the multiple source systems there are *n* current sources, one for each electrode. The system operates by applying *patterns* of currents, where a pattern defines the current source value for each electrode. The sum of the currents applied to the electrodes must equal zero.

In the modern EIT systems the reference sinusoidal waveform is produced by digital waveform synthesis techniques. There are two ways of sinusoidal digital synthesis. The first consists of storing the points of a sinusoid (all or 1/4) in a PROM and sequentially stepping through these stored values. The second way is to use a direct digital synthesizer (DDS) integrated circuit (e.g., AD9831). In both cases, an analog waveform is produced by feeding the digital samples through a digital-to-analog converter.

Current sources

The current source in an EIT system must be able to deliver current with a desired precision over a specified frequency range to load impedances within an expected range of values [4,13]. These requirements specify the frequency response, output impedance and voltage compliance of the current source. In medical applications with single sinusoid excitation, rms current values are in the range 1÷5 mA, with smaller current values being used at lower frequencies because of safety reasons. The load impedances are typically within the range from 100 Ω to 10 kΩ. These are a function of electrode size, excitation frequency and the tissue being imaged, with the lower values observed at higher frequencies. These values of the currents and impedances require voltage ranges of a few volts.

The output impedance of the current sources has to be greater than 1 MΩ in the whole operating frequency range (usually 10 kHz – 1 MHz). In order to have 0.1 % accuracy of the specified current (as required for the multiple source systems with optimal current patterns), 12 or 16-bits DACs have to be used.

The current sources used in the modern EIT systems are in fact voltage-to-current converters, since they produce an output current that is proportional to an input voltage. An ideal current source must have an infinite output impedance, Z_0, resulting in the current delivered to the load being independent of the load voltage. Real current sources, however, have a finite Z_0.

Multiple current source systems generally require current sources with precision higher than the precision of single source systems. The reason is that it is necessary to keep common-mode current (the sum of all currents), negligibly small.

One of the most often used current sources in EIT is the Howland current source, shown in fig. 5 [4]. An alternative implementation of the Howland source uses an instrumentation amplifier instead the usual inverting amplifier. For an ideal operational amplifier (OA), the output impedance of the source is infinite when the resistors satisfy the relationship

$$R_4 / R_3 = R_2 / R_1 \tag{22}$$

At this condition the load current can be expressed as

$$I_L = -V_{in} / R_3 \tag{23}$$

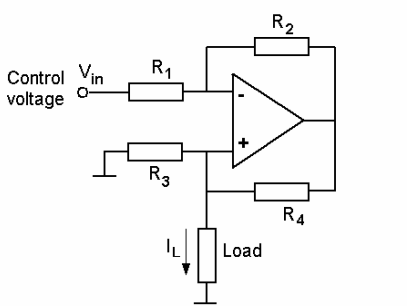

Fig. 5 - *Howland current source*

The primary advantages of the Howland current source are its simplicity and ability to produce high output impedance with the appropriate trimming. In practice, however, the non-ideal OA behavior results in a non-zero output capacitance. There are two ways to compensate for the output capacitance - inserting a negative capacitance and creating a parallel *LC* circuit by introducing an inductor. A negative capacitance can be synthesized using a negative impedance converter (NIC). The second way is to create an *LC* resonant circuit by introducing a parallel inductance, synthesized using a gyrator. Gyrators (or generalized impedance converters - GIC) are mostly used in the design of active filters.

Synchronous voltmeters

EIT systems that reconstruct the distribution of both conductivity and permittivity require measurement of the real and reactive voltages on the electrodes. If the load is resistive, the EIT systems require phase-sensitive voltage measurements in order to extract the real part of the electrode voltage. Measuring the magnitude of the electrode voltage would result in greater sensitivity to stray capacitance. These phase-sensitive measurements are made using a synchronous voltmeter that uses a coherent reference obtained from the waveform generator. An analog implementation of a phase-sensitive voltmeter is shown in fig. 6.

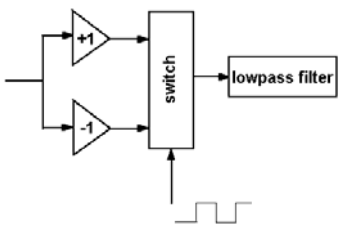

Fig. 6 – *Analog synchronous voltmeter*

A reference square wave having the exact frequency as the input sinusoidal waveform is used to control a switch that alternately applies non-inverted and inverted input signal to a lowpass filter. The square wave is supplied by the waveform synthesis block, which also produces the

system excitation waveform, to ensure that the frequencies of the two signals are the same. The relative phase of the reference signal determines whether the voltmeter measures the real voltage, reactive voltage, or a combination of the two. Adjusting the reference phase to maximize the output with a resistive load can be used to determine the set of appropriate reference waveform phases to measure the real voltage. The synchronous voltmeter of fig. 6 mixes the input signal with a square wave of the same frequency and keeps the DC part of the result. Integrated circuits such as AD630 are able to perform this operation. Practically, the synchronous voltmeter includes high input impedance buffer, variable gain amplifier, synchronous demodulator, low-pass filter and analog to digital converter.

As the analog ICs have some drawbacks, the modern EIT systems perform synchronous voltage measurement using digital synchronous voltmeters, usually implemented by digital signal processors (DSP) to obtain the real and reactive voltage values.

Measuring voltages from the current-carrying electrodes causes problems in image reconstruction since the contact impedances between electrodes and tissue are not known. If static images are needed, the unknown contact impedances produce large artifacts. The contact impedance problem can be avoided by using the so-called *compound electrodes* (fig. 7) in which the current injection and voltage measurements are made from different parts of the electrode that are not in connection with each other.

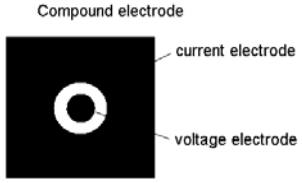

Fig. 7 - *Compound electrode*

4. RECENT ADVANCES IN EIT

4.1 3D EIT

In most practical cases of biomedical imaging the problem is three dimensional. Till recently most of the published works considered 2D reconstructions. This was because of the following reasons:

- The 3D problem requires larger mesh and more extended time to solve the forward and the inverse problem. So, faster computers and better numerical algorithms are needed.
- The more are the individual elements in which the conductivity is sought, the more must be the independent measurements and more complicated must be the current injection patterns. This requires higher number of electrodes and creates difficulties with their placement (must be very miniature) and also increase the time for data collection, which requires higher speed data acquisition system.
- In some typical cases the 2D reconstruction gives good results.
- It was easier to check new and improved algorithms for EIT image reconstruction on simple 2D objects for which there were many numerical and experimental data for comparison.

Nowadays, the speed of the present computers is sufficiently high to solve quickly 3D problems with moderate number of elements (about 10000), and the available electronics is faster and cheaper. Dual-core 64-bits processors promise considerable speed-up in solving the 3D forward and inverse problems, and even 4- and 8-core processors can be found on the market. The parallel numerical processing promises very good perspectives even for 3D imaging in real time.

The problem still remaining is the one with the higher number of electrodes - their miniaturization and the complexity of data collection will probably be solved in the following years.

4.2 Forward solvers

In order to achieve an accurate EIT image reconstruction, it is necessary to have a model capable of predicting accurately the electrode voltages for a given conductivity distribution. The conductivity is adjusted by the Gauss-Newton algorithm until the electrode voltages fit to the measurement precision. It is clear that the voltages on the electrodes must be predicted with a precision better than the accuracy of the measurements. Such precision of the numerical simulation can be provided by the Finite Element Method. It is very suitable for solution of the forward problem in EIT, as the explored media in EIT are non-homogeneous and the geometries of the regions are irregular. The application of the FEM leads to symmetric, positive definite sparse matrices. For 2D problems, a standard approach to solve the linear system resulting from the finite element discretization is to employ direct method - Cholesky or LU decomposition, together with forward and backward substitution. Sparse matrix variants of these methods are usually used, together with suitable node renumbering.

In 3D, the iterative solution methods have become more attractive, although each iterative step must be applied for each current pattern. Iterative methods also have an advantage that the number of iterations needed to solve the forward solution can be reduced as the iteration can be initialized with the previously computed values.

For the conductivity reconstruction in 3D, the conjugate gradient method is a favorite choice [6]. Its convergence is improved using a preconditioner - usually an approximate inverse of the system matrix. If the conductivity does not vary too much during the reconstruction process, the approximate inverse can be precomputed for a typical initial conductivity. For the complex admittivity reconstruction the GMRES algorithm can be used.

Iterative methods can save computing time if the solution is not required to full machine precision. Because the boundary voltages are not so accurately measured, it is unnecessary to solve the forward problem to the full accuracy.

In the last years higher order elements are also used, which allows a higher accuracy of potential and voltage computation with lower number of elements. This is favorable for solving the inverse problem because if the elements with different conductivities are less, a lower number of independent measurements will be necessary. Despite the efforts in this field, the best choice of finite elements for EIT remains still an open problem.

The possibility of using vector elements is also promising, especially for 3D problems.

4.3 Adaptive mesh refinement

A fruitful strategy for reducing the solution time and for increasing the accuracy of reconstruction is to adaptively vary the finite element mesh. During the forward solution at fixed conductivities, the mesh density is increased where high electric field intensities are found, and decreased, where the potential is varying slow. This results in a more accurate solution than using a regular mesh. One complexity exists here, because the problem is solved at multiple right-hand sides – the fields will be different for every excitation pattern and the meshes have to be also different, so the forward problem must be solved entirely for each current pattern. Otherwise, using the same mesh in each pattern, the factored matrix is the same and only forward and backward substitution must be repeated for each current pattern.

The adaptive mesh refinement is used in [7] to locally adapt the mesh where the reconstruction algorithm indicates large gradients in conductivity. The advantages of tuning the element density adaptively at solution time are even greater in 3D EIT .

Another attractive approach is to solve first on a coarse grid to give the crude features of a solution which is then extrapolated to a finer grid where a more accurate solution is calculated. A systematic treatment of this switching between finer and coarser grids is used in multigrid solution algorithms.

4.4 Parallel processing

A possibility for accelerating the solution of the inverse EIT problems exists using the property that the FEM solutions for the different current patterns are to a great extent independent of each other. They have the same system matrix, but different right hand sides, corresponding to different current patterns. Thus, the system matrix can be assembled and factored by the master processor and spread to the slave processors of a master-slave parallel system for back-substitution with different right-hand sides. The slave processors compute the rows of the Jacobian belonging to separate current patterns and return them back to the master processor that assembles the whole Jacobian and solves Eq. (20) for the *k*-th iteration. In 3D problems there will be much more different current patterns and savings will be higher.

The Hessian matrix $\mathbf{J}\mathbf{J}^{\mathbf{T}}$ in (20) is full and dense, thus requiring considerable efforts to solve. There are possibilities not to form this matrix explicitly. The Hachtel's augmented matrix method improves the accuracy of the solution since the augmented matrix has a condition number lower than that of the original Hessian. This method is faster because it is not necessary to explicitly compute the Hessian matrix and the augmented matrix is sparse. It can be solved easily by iterative methods that are easily parallelizable, e.g., the conjugate gradient method.

The parallel processing can be implemented using MPI libraries for cluster of computers, or using OpenMP directives of modern C++ and Fortran 90 compilers, for multicore processors that are nearly omnipresent nowadays. The users of Matlab package could consider using the Distributed computing toolbox, which gives the end users good possibilities to use parallel processing without heavy programming.

4.5 Optimal current patterns

The spatial resolution of an EIT system can be improved using bigger number of electrodes, in order to increase the pixels with different conductivities in the image. Quantitative measure of the ability of a current pattern I to distinguish two different conductivity distributions σ_1 and σ_2 can be introduced using the voltage difference $\|R(\sigma_1)I - R(\sigma_2)I\|_\infty$ to be greater than the measurement precision ε. This voltage difference must be constrained by the sum of the currents because of the present safety regulations (also, the maximum magnitude of the currents or/and the power can be constrained). $R(\sigma)$ is the resistance matrix for the conductivity distribution σ.

The *distinguishability* δ of σ_1 from σ_2, when using a current pattern *I,* can be defined as:

$$\delta(I) = \frac{\|R(\sigma_1)I - R(\sigma_2)I\|}{\|I\|} \tag{24}$$

where $R(\sigma)I$ denotes the voltage on the boundary $\delta\Omega$ resulting from the application of the current pattern I to a body having the conductivity distribution σ.

It was shown in [14] that in order to improve resolution by increasing the number of electrodes, one should apply currents to all the electrodes. For this reason many modern EIT systems use as many current generators as electrodes. Other result also implies that EIT systems should use large electrodes that fill as much of $\delta\Omega$ as possible, to make the current densities more homogeneous.

In order to find the best current pattern for distinguishing σ_1 from σ_2, the following adaptive process can be used [14]:

1) Guess a current pattern I_0 for which $\int_{\delta\Omega} I_0 = 0$ and $\|I_0\| = 1$. Set $k = 0$.

2) Measure the voltage on $\delta\Omega$:

$$V_k^1 = R(\sigma_1)I_k$$

3) Compute the voltage on $\delta\Omega$:

$$V_k^0 = R(\sigma_2)I_k$$

4) Compute the new estimate I_{k+1} to the best current density by

$$I_{k+1} = \frac{V_k^1 - V_k^0}{\left\| V_k^1 - V_k^0 \right\|}$$

5) If the change in I is less than the measurement precision ε,

$$\left\| I_{k+1} - I_k \right\| < \varepsilon$$

then stop; otherwise increment k and repeat, starting with step 2.

This algorithm is essentially the power method for finding the largest eigenvalue and corresponding eigenvector of a matrix. Numerical and experimental tests of this adaptive process by 32-electrode EIT system [14] have shown about 30-fold improvement in distinguishability within 5 iterations.

For a multi-current-generator system, the question is which current density patterns should be used in order to best distinguish between two conductivity distributions σ_1 and σ_2. It is said that the current pattern I is the "best" pattern for distinguishing σ_1 from σ_2 if I maximizes the distinguishability δ. A simple example exists of distinguishing a homogeneous annulus with conductivity σ_1 from a homogeneous disk with conductivity σ_2. In this case, the eigenfunctions of $\left| R(\sigma_1) - R(\sigma_2) \right|$ are trigonometric functions and the best current pattern is therefore simply the trigonometric pattern $I(\theta) = I_m \cos(\theta - \theta_0)$ for any θ_0.

If the conductivity σ is not rotationally invariant, then the cosine is not necessarily the best current density to distinguish σ_1 from a homogeneous conductivity σ_2. In general, since the best current densities depend on the unknown conductivity σ inside the body, they cannot be known in advance. They can be determined, however, by the adaptive process shown above.

In the standard implementation of this algorithm, an initial current pattern is set, its voltage response is measured from the real object, and its voltage response for the estimated conductivity distribution is calculated. Then, the voltage difference is calculated and normalized, and is used as the updated current pattern. Eventually, the current pattern will converge to the eigenvector. This procedure requires no advance knowledge of the conductivity distribution and is numerically stable. However, it does require repetitive measurements from the real object and lengthy acquisition time. It is shown however, that updating optimal currents every few reconstruction iterations improves the image quality in an iterative reconstruction algorithm.

The optimal current injection strategy produces the most uniform sensitivity and therefore the most accurate images, but in practice there are some drawbacks of this method. Optimal current patterns use all electrodes for the current injection and need as many current generators as there are electrodes. This makes the measurement system comparatively complicated.

The trigonometric current excitation is also useful for moving the axis of the rotating electric field without commutation, in small steps. In this way, a larger number of independent measurements are obtained and the accuracy of the solution of the inverse problem is improved. In this approach the current sources must have voltage controlled amplitudes, according to the formula:

$$I_k = I_m \cos(\theta_k - \theta_0) \qquad (25)$$

where I_m is the amplitude of the current, θ_0 is the desired direction of the current density vector, and θ_k are the angular positions of the midpoint of electrode k.

The trigonometric excitation leads to sensitivity matrices (Jacobians) that are better conditioned and more robust against noise. This improves the spatial resolution at a reasonable complexity of the current generators.

Using trigonometric excitation, different current patterns can be obtained, corresponding to higher order space harmonics. Thus, for inhomogeneities near the surface, higher order space harmonics can be used, because they push the current near the surface. For inhomogeneities near the center, the first space harmonic can be used, because it ensures nearly constant current density in the whole volume, including the center.

On figs. 8, 9, 10, 11, the first, second and third space harmonics are shown:

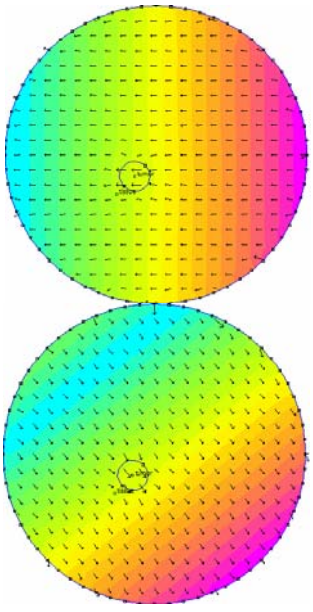

Fig. 8 - 1st harmonic (a)

Fig. 9 - 1st harmonic (b)

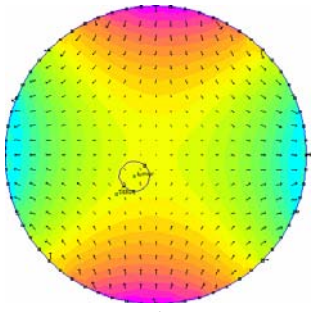

Fig. 10 - 2nd harmonic

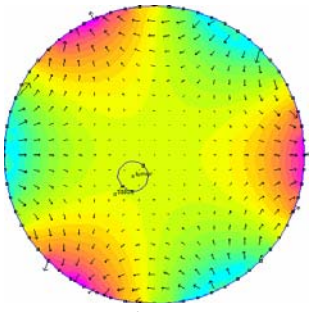

Fig. 11 - 3rd harmonic

5. EXAMPLES OF EIT RECONSTRUCTIONS

In the first example the position of a tumor (σ=*1 S/m, r=1 cm*) inside circular region with normal tissue *(σ=0.1 S/m, r=10 cm)* is sought (fig. 12). 32 electrodes are placed on the surface of the region. 16 pairs of opposite excitations are applied, specifying current of 1 mA. The number of the unknown conductivities is 476 and the number of independent measurement points is *np = 32.16 = 512*. The solution of the inverse problem – the conductivities in every element represented as color picture, is shown on fig. 12. It is seen from fig. 12 that the reconstructed tumor region has bigger diameter than the real one. This is due to the comparatively large size of the elements used. Further improvement of the accuracy of reconstruction is possible using adaptive mesh refinement of the regions with high gradients of the conductivities. After one step of refinement of the mesh the result is shown on Fig. 13. The improved accuracy of reconstruction is clearly visible.

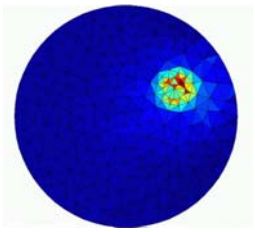

Fig. 12 - *without refinement*

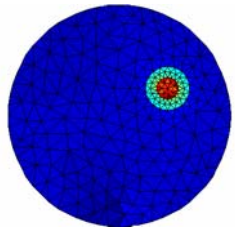

Fig. 13 - *with refinement*

The second example on fig. 14 is similar, but this time a trigonometric excitation is used. The place of the tumor is clearly visible on fig. 15. The size of the tumor is somewhat exaggerated.

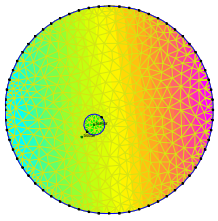

Fig. 14 - Another case

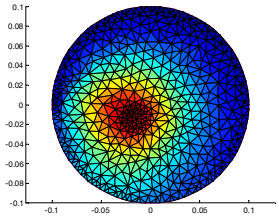

Fig. 15 – *the image*

The third example is a 3D example, shown on figs. 16-19, obtained with the popular software package EIDORS 3D [12]. EIDORS 3D is a fairly complete reconstruction program, written in the Matlab language. It is freely available software that can be used to reconstruct material conductivities and admittivities from boundary measurements. The finite element method for the forward calculations is used. The regularized Gauss-Newton method for obtaining a stable inverse solution is implemented. It is free software that can be easily modified to implement new algorithms and methods. Its drawback is the slow execution speed, as the Matlab language is an interpretative language. This package is of order of magnitude slower than applications obtained by using optimized C, C++ or Fortran 90 compilers. Of course, using the Matlab compiler can speed up the package, but it cannot compete with the optimized compilers. For this reason the author of this paper developed a Fortran 90 reconstruction program based on Gauss-Newton method, that has improved speed and is easily parallelizable using OpenMP on dual-core and multi-core processors.

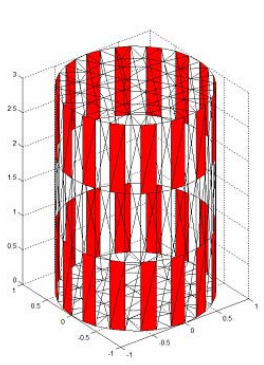

Fig. 16 - *electrodes*

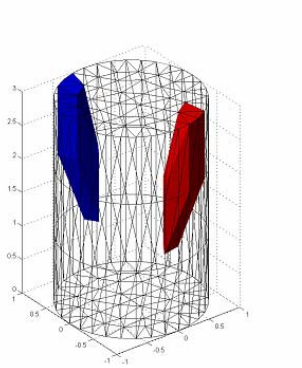

Fig. 17 - *inhomogeneities*

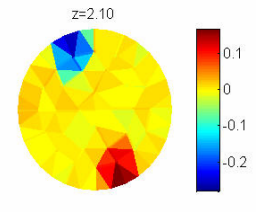

Fig. 18 - *Results at z=2.1*

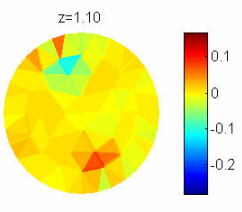

Fig. 19 - *Results at z=1.1*

6. CONCLUSIONS

The basic algorithm, instrumentation and advances of EIT are reviewed here. Many problems still remain to be solved before EIT becomes a practically useful method. The challenges can be classified into the areas of electronics, algorithms, and clinical and industrial applications. Because the problem is inherently ill-posed, the measurements must be made very accurately. Thus, the improvement of instrumentation accuracy is very important. For clinical applications, the measurements must be made very quickly, in real time. Also, to obtain good images, too many electrodes should be used to improve the spatial resolution. The ill-posedness and nonlinearity of the reconstruction problem requires advanced iterative methods, new regularization techniques and very fast solvers. The non-iterative methods are also important, especially for real-time clinical applications.

The ill-posedness of the EIT inverse problem is a main reason not to expect from it a resolution comparable to that of computer tomography or magnetic resonance imaging. Nevertheless, EIT devices are safe, low cost, and portable, that will ensure them a deserved place in the medical and industrial applications.

REFERENCES

[1] J. Webster: "*Electrical Impedance Tomography"*, Adam Hilger, 1990.

[2] M. Cheney, D. Isaacson and J. Newell: "Electrical Impedance Tomography", SIAM Review, 1999, Vol. 41, No. 1, pp.85-101.

[3] W. Lionheart: "EIT reconstruction algorithms: pitfalls, challenges and recent developments", Physiol. Meas., 25, 2004, pp. 125–142.

[4] D. Holder: "*Electrical Impedance Tomography"*, 1st ed., Institute of Physics Publishing, Bristol and Philadelphia; 2005.

[5] R. Yerworth, R. Bayford, G. Cusick, M. Conway, D. Holder: "Design and performance of the UCLH Mark 1b 64-channel electrical impedance tomography (EIT) system, optimized for imaging brain function", Physiol. Meas. **23,** 2002, pp. 149–158.

[6] N. Polydorides: "*Image reconstruction algorithms for soft field tomography*", PhD Thesis, UMIST, 2002.

[7] M. Molinari, B. Blott, S. Cox and G. Daniell: "Optimal imaging with adaptive mesh refinement in electrical impedance tomography", Physiol. Meas. **23**, 2002, pp. 121–128.

[8] M. Vauhkonen, "*Electrical Impedance Tomography and Prior Information"*. PhD thesis, University of Kuopio, Kuopio, Finland, 1997.

[9] M. Vauhkonen, W. Lionheart, L. Heikkinen: "A Matlab package for the EIDORS project to reconstruct two-dimensional EIT images", Physiol. Meas*.* **22,** 2001, pp. 107–11.

[10] M. Molinary, S.J. Cox, B.H. Blott, and G.J. Daniell, "Efficient Non-linear 3D Electrical Tomography Reconstruction", 2nd World Congress on Industrial Process Tomography*,* 29-31 August 2001, Hannover, Germany, pp. 424-432.

[11] A. Borsic: "*Regularization methods for imaging from electrical measurements"* , PhD Thesis, Oxford Brookes University, 2002.

[12] N. Polydorides, W. Lionheart: "A Matlab toolkit for three-dimensional electrical impedance tomography: a contribution to the electrical impedance and diffuse optical reconstruction software project" Meas. Sci. Technol*.* **13** 2002, pp. 1871–83.

[13] A. Ross, G. Saulnier, J. Newell, D, Isaacson: "Current source design for electrical impedance tomography", Physiol. Meas. **24** , 2003, pp. 509–516.

[14] D. Gisser, D. Isaacson, J.Newell: "Theory and performance of an adaptive current tomography system". Clin. Physiol. Meas. 9, Suppl. A (1988), pp. 35-41.

K. Brandisky was born in the city of Plovdiv, Bulgaria, on 06.11.1950. He obtained the degree of Electrical Engineer in Radioelectronics from TU-Sofia, Sofia, Bulgaria in 1973. In 1983 he received the PhD degree in electrical engineering from TU-Sofia, with main field of study - computational electromagnetics.

He worked as Assistant Professor at the Department of Theoretical Electrical Engineering, TU-Sofia from 1976 till 1989 and then, from 1989-2006, as Associate Professor. From 1992-1994 he worked as postdoctoral research fellow at KU Leuven, Belgium. His research interests are in the computational electromagnetics and finite element method, optimization of electromagnetic devices and inverse problems for electrical impedance tomography.